

Warm-Electron Effects in *n*-Type Silicon and Germanium

M. H. JØRGENSEN

Physics Laboratory III, The Technical University of Denmark, Lyngby, Denmark

(Received 20 October 1966)

The Boltzmann equation describing the warm-electron case is discussed and a review is given of the scattering mechanisms for *n*-Ge and *n*-Si with relatively low doping levels. Taking into account the known band structure, the Boltzmann equation is solved by a numerical iteration method under the assumption of weak intervalley scattering. It is shown that this condition can be relaxed for special symmetry directions. The warm-electron coefficient β has been measured in the temperature range from 77 to 250°K by an audio-frequency method based on analysis of nonlinear distortion. Good agreement between measured and calculated results is obtained using the accepted values of the deformation-potential constants.

I. INTRODUCTION

APPLICATION of high electric fields to homogeneous semiconductor crystals gives rise to fundamental deviations from Ohm's law. Such a nonlinear relationship between current and voltage was first observed in germanium by Ryder and Shockley.¹ Qualitatively the effect is simple to describe. The electrons are accelerated in the electric field such that their mean energy $\langle \epsilon \rangle$ is increased in comparison to the thermal equilibrium energy ϵ_L . Departures from Ohm's law then occur when the momentum relaxation time is energy-dependent.

The electrical characteristic as a function of electric field is conveniently divided into three regions: (a) the warm-electron region (low electric fields), (b) the region of intermediate fields, and (c) the hot-electron region (high electric fields). More specifically, in the warm-electron region the difference $\langle \epsilon \rangle - \epsilon_L$ is small compared to ϵ_L and only the second-order term in the electric field F in a power-series expansion of μ is important.^{2,3} In the hot-electron region $\langle \epsilon \rangle$ is large compared to ϵ_L and striking deviations from Ohm's law are often found (current saturation). It should be stressed that we do not consider field-induced variations in the free-carrier concentration (secondary ionization, etc.) in the present treatment.

For experiments on warm- and hot-electron effects one can, in principle, obtain information about the scattering of electrons by phonons, impurities, and other free carriers. Investigations of this type may yield quantitative information about the mechanism of energy and momentum relaxation. Also, it is, of course, of fundamental interest to have a quantitative description of these nonlinear effects.

Several attempts have been made to draw quantitative conclusions about the scattering parameters from hot-electron experiments, especially in *n*-type germanium and silicon.⁴⁻⁶ Recently it has been pointed out,

however, that the assumptions made in these investigations (constant effective mass, neglecting secondary minima in the conduction band, etc.) are not realistic.^{7,8}

A demonstration of the importance of the detailed band structure is found in the case of GaAs.⁹ These complications make the hot-electron experiments less useful for quantitative investigations on the scattering parameters.

In the warm-electron case on the other hand, the electrons stay close to the conduction-band minima and these secondary effects may be neglected. Also the warm-electron coefficients⁸ β_0 and γ_0 are strongly dependent on the scattering parameters. With a complete theory for the warm-electron effect we thus have a very sensitive method for determining the magnitudes of these parameters.

A number of theoretical and experimental investigations have been concerned with warm-electron effects in Ge and Si.¹⁰⁻¹³ Most of the theoretical treatments have, however, made so many simplifying assumptions, as to prevent a detailed comparison with experiment. In some instances a spherical energy band has been used instead of the established many-valley structure.^{10,11} Also, simplifying assumptions have been introduced concerning the form of the electronic energy-distribution function (e.g., Refs. 12, 13, and 14). Scattering by optical phonons has frequently been neglected.¹⁵⁻²⁰ In a realistic model we must take into account the many-

⁷ M. Cardona, W. Paul, and H. Brooks, *Helv. Phys. Acta* **33**, 329 (1960).

⁸ N. I. Meyer and M. H. Jørgensen, *J. Phys. Chem. Solids* **26**, 823 (1965).

⁹ A. R. Hutson, A. Jayaraman, A. G. Chynoweth, A. S. Coriell, and W. L. Feldman, *Phys. Rev. Letters*, **14**, 639 (1965).

¹⁰ I. Adawi, *Phys. Rev.* **120**, 118 (1960).

¹¹ J. Yamashita, *Phys. Rev.* **111**, 1529 (1958).

¹² H. Sato, *J. Phys. Soc. Japan* **14**, 1275 (1959).

¹³ K. H. Seeger, *Z. Physik* **156**, 582 (1959).

¹⁴ M. S. Sodha and D. B. Agarwal, *Can. J. Phys.* **36**, 707 (1958).

¹⁵ I. M. Dykman and P. M. Tomchuk, *Fiz. Tverd. Tela* **2**, 2228 (1960) [English transl.: *Soviet Phys.—Solid State* **2**, 1988 (1961)].

¹⁶ M. Hattori and H. Sato, *J. Phys. Soc. Japan* **15**, 1237 (1960).

¹⁷ M. S. Sodha, *Phys. Rev.* **107**, 1266 (1957).

¹⁸ M. S. Sodha and P. C. Eastmann, *Phys. Rev.* **110**, 1314 (1958).

¹⁹ M. S. Sodha and Y. P. Varshni, in *Proceedings of the International Conference on Semiconductor Physics, 1960* (Czechoslovakian Academy of Sciences, Prague, 1961).

²⁰ J. Yamashita and M. Watanabe, *Progr. Theoret. Phys.* (Kyoto) **12**, 443 (1954).

¹ E. J. Ryder and W. Shockley, *Phys. Rev.* **81**, 139 (1951).

² J. B. Gunn, *Progr. Semicond.* **2**, 213 (1957).

³ K. J. Schmidt-Tiedemann, *Phys. Rev.* **123**, 1999 (1961).

⁴ H. G. Reik and H. Risken, *Phys. Rev.* **124**, 777 (1961).

⁵ H. G. Reik and H. Risken, *Phys. Rev.* **126**, 1737 (1962).

⁶ M. H. Jørgensen, N. I. Meyer, and K. J. Schmidt-Tiedemann, in *Proceedings of the International Conference on the Physics of Semiconductors, Paris, 1964* (Academic Press Inc., New York, 1964), p. 457.

valley structure, the anisotropic effective mass, and intervalley scattering in addition to intravalley scattering and the anisotropic impurity scattering. Recently a treatment including most of these features has been published by Tsutsumi,²¹ who presents formal expressions for a number of higher-order galvanomagnetic transport coefficients. No attempt was made, however, to extract the warm-electron parameters from the general expressions or to numerically evaluate these so as to permit a comparison with experimental results.

In the present paper an alternative approach to solving the Boltzmann equation is presented. It is based on a simple numerical-iteration method and it leads to results for the warm-electron parameters which are directly amenable to comparison with experimental results. The most important limitation in our treatment is the assumption that the intervalley scattering is weak compared to the intravalley scattering. This is fulfilled in germanium, whereas in silicon it only applies in some special cases. We, furthermore, assume that the impurity concentration is sufficiently small so that electron-electron scattering can be neglected.

Experimental results on warm electrons have been obtained by dc pulse methods for Ge^{2,22} and by microwave methods for Ge²³⁻²⁷ and Si.^{26,27}

We have measured the warm-electron coefficients for *n*-type Ge and Si by a technique based on the harmonic signal generation at audio frequencies.^{28,29} The measurements were carried out in the temperature range 77 to 250°K.

Comparison between our calculated and measured results shows very good agreement both with regard to temperature variation and to the absolute values of the parameters when using the accepted deformation potential constants in the calculations.

The formal warm-electron theory is summarized in Sec. II. The appropriate transport equation is set up in Sec. III and the general form of the distribution function is discussed. The different scattering mechanisms are explicitly introduced in Sec. IV, while the method of solution of the transport equation is described in Sec. V. β_0 and γ_0 are derived in Sec. VI. A short description of the experimental arrangement is given in Sec. VII. Experimental data are presented and compared with the theoretical results in Sec. VIII.

II. FORMAL WARM-ELECTRON THEORY

In this section a short discussion of the warm-electron parameters β_0 and γ_0 will be given.

At low electric fields we have the following relation between current density \mathbf{J} and field \mathbf{F} in a perfect crystal³:

$$J_i = \sigma_0(F_i + \sum_{jkl} h_{ijkl} F_j F_k F_l), \quad (1)$$

where terms of the fifth and higher orders have been neglected. (Because of symmetry only odd terms in \mathbf{F} will occur.) σ_0 is the scalar zero-field conductivity.

Schmidt-Tiedemann has shown that the tensor h_{ijkl} for a crystal of cubic symmetry can be completely described by only two independent parameters³:

$$\beta_0 = h_{1111} \quad \text{and} \quad \gamma_0 = h_{1111} - 3h_{1122}. \quad (2)$$

Denoting the current component in the field direction by J_L , we have³

$$J_L = \sigma_0 F(1 + \beta F^2), \quad (3)$$

where β depends on the field orientation (longitudinal anisotropy):

$$\beta = \beta_0 - \gamma_0(1 - \sum_i e_i^4). \quad (4a)$$

The unit vector \mathbf{e} is defined by $\mathbf{F} = F\mathbf{e}$.

The interpretation of warm-electron experiments is usually simplified by choosing a sample orientation such that \mathbf{F} and \mathbf{J} are parallel to a $\langle 110 \rangle$ plane in the crystal. Using this special geometry, β can be expressed in terms of the angle α ³ (Fig. 1):

$$\beta = \beta_0 - \frac{1}{16}\gamma_0(7 - 4\cos 2\alpha - 3\cos 4\alpha). \quad (4b)$$

In general \mathbf{J} and \mathbf{F} will have different orientations (transverse anisotropy or Sasaki effect). The anisotropy angle ψ defined in Fig. 1 depends only on γ_0 and α ³:

$$\tan \psi = F^2 \gamma_0 \frac{1}{16} (2 \sin 2\alpha + 3 \sin 4\alpha). \quad (5)$$

The experimental values of β_0 and γ_0 are usually determined from Eq. (4b). γ_0 may, however, be found if Eq. (5) is applied to low-field measurements of the Sasaki effect.³⁰

Now we shall turn to the theoretical calculation of β_0 and γ_0 , where the main problem is to determine the appropriate distribution function for the electrons. From the distribution function one finds J_L as a function of F , which by comparison with Eqs. (3) and (4) gives the desired expressions for β_0 and γ_0 .

²¹ O. Tsutsumi, J. Phys. Soc. Japan **19**, 1290 (1964).

²² J. B. Gunn, J. Electron. **2**, 87 (1956).

²³ T. N. Morgan, J. Phys. Chem. Solids **8**, 245 (1959).

²⁴ T. N. Morgan and C. E. Kelly, Phys. Rev. **137**, A1573 (1965).

²⁵ J. B. Arthur, A. F. Gibson, and J. W. Granville, J. Electron. **2**, 145 (1957).

²⁶ M. A. C. S. Brown, J. Phys. Chem. Solids **19**, 218 (1962).

²⁷ C. Hamaguchi and Y. Inuishi, J. Phys. Soc. Japan **18**, 1755 (1963).

²⁸ T. Guldbrandsen, N. I. Meyer, and J. Schær-Jakobsen, Rev. Sci. Instr. **36**, 743 (1965).

²⁹ M. H. Jørgensen and N. I. Meyer, Solid State Commun. **3**, 311 (1965).

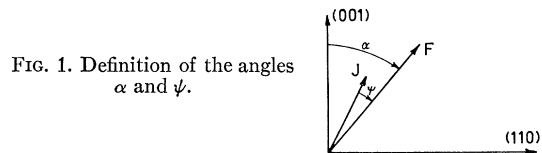


FIG. 1. Definition of the angles α and ψ .

³⁰ M. H. Jørgensen, N. I. Meyer, and K. J. Schmidt-Tiedemann, Solid State Commun. **1**, 226 (1963).

III. BOLTZMANN EQUATION

We shall first consider the electrons in one of the equivalent valleys in the conduction band of Ge or Si. The effective mass tensor is³¹

$$\mathbf{m} = \begin{Bmatrix} m_t & 0 & 0 \\ 0 & m_t & 0 \\ 0 & 0 & m_l \end{Bmatrix}.$$

The fundamental Boltzmann equation for the electronic distribution function $f(\mathbf{k})$ reads

$$\left(\frac{\partial f}{\partial t}\right)_{sc} + \frac{e}{\hbar} \mathbf{F} \cdot \text{grad}_{\mathbf{k}} f = 0, \quad (6)$$

where the first term accounts for the scattering processes. The distribution function is expanded in the usual form:

$$f(\mathbf{k}) = f_0(\epsilon) + \mathbf{g}(\epsilon) \cdot (\mathbf{k} - \mathbf{k}_0), \quad (7)$$

where \mathbf{k}_0 is the wave vector corresponding to the energy minimum of the valley under consideration. From a mathematical point of view, the use of Eq. (7) corresponds to expanding $f(\mathbf{k})$ in spherical harmonics, keeping terms of zeroth and first order only.

The scattering anisotropy is taken into account by defining an energy-dependent momentum-relaxation-time tensor:

$$\boldsymbol{\tau}(\epsilon) = \begin{Bmatrix} \tau_t(\epsilon) & 0 & 0 \\ 0 & \tau_t(\epsilon) & 0 \\ 0 & 0 & \tau_l(\epsilon) \end{Bmatrix},$$

(following the theory of Herring and Vogt³¹). So long as the relaxation time approximation is valid³¹ we have

$$(\partial \mathbf{g} / \partial t)_{sc} = -\boldsymbol{\tau}^{-1} \cdot \mathbf{g}. \quad (8)$$

In order to simplify the notation we now define a mobility-anisotropy tensor by

$$\boldsymbol{\Omega} = (m_l / \tau_l) \mathbf{m}^{-1} \cdot \boldsymbol{\tau}. \quad (9)$$

This can be written in the more explicit form

$$\boldsymbol{\Omega} = \begin{Bmatrix} 1 & 0 & 0 \\ 0 & 1 & 0 \\ 0 & 0 & 1/K \end{Bmatrix}, \quad (10)$$

if we introduce the mobility-anisotropy coefficient

$$K = \left(\frac{m_l}{m_t}\right) \left(\frac{\tau_t(\epsilon)}{\tau_l(\epsilon)}\right). \quad (11)$$

K is, in principle, energy-dependent when different scattering mechanisms are mixing, but it can be shown that it only varies slightly with energy in most cases of interest here. Also, it turns out that the whole theory becomes much simpler if K is considered as a constant. We shall adopt this approximation in the following.

The fundamental Boltzmann equation can be developed a few steps further. Inserting (7) and (8) into (6) and separating odd and even terms in $(\mathbf{k} - \mathbf{k}_0)$ one obtains two new equations:

$$\mathbf{g}(\epsilon) = e\hbar \frac{\tau_t(\epsilon)}{m_t} \frac{df_0}{d\epsilon} \boldsymbol{\Omega} \cdot \mathbf{F}, \quad (12)$$

$$0 = \left(\frac{\partial f_0}{\partial t}\right)_{sc} + \frac{2e^2}{3m_t} \epsilon^{-1/2} (\mathbf{F} \cdot \boldsymbol{\Omega} \cdot \mathbf{F}) \times \frac{d}{d\epsilon} \left(\epsilon^{3/2} \tau_t(\epsilon) \frac{df_0}{d\epsilon} \right). \quad (13)$$

Equation (13) is the warm-electron Boltzmann equation which we shall solve for f_0 . If $f_0(\epsilon)$ is known, the drift velocity in the valley under consideration can be deduced from (12). From simple calculations we get the well-known result

$$\mathbf{V}_d = \frac{2e}{3m_t} \boldsymbol{\Omega} \cdot \mathbf{F} \frac{\int_0^\infty \epsilon^{3/2} \tau_t(\epsilon) / (df_0/d\epsilon) d\epsilon}{\int_0^\infty \epsilon^{1/2} f_0(\epsilon) d\epsilon}. \quad (14)$$

In the case of nondegenerate statistics, Eq. (13) has for $F=0$ the solution

$$f_0(\epsilon) = C_0 \exp(-\epsilon/kT), \quad (15)$$

which makes

$$\left(\frac{\partial f_0}{\partial t}\right)_{sc} = 0.$$

At low fields we can write the general solution to (13) in the form

$$f_0(\epsilon) = C_0 \exp(-\epsilon/kT) + (\mathbf{F} \cdot \boldsymbol{\Omega} \cdot \mathbf{F}) \Phi(\epsilon) \quad (16)$$

(neglecting terms of fourth and higher order in F). By inserting (16) into (14) one obtains the characteristic quadratic deviations in F from Ohm's law.

IV. SCATTERING MECHANISMS

Before a more specific treatment of the Boltzmann equation can be given, we must discuss the relevant scattering mechanisms with special emphasis on a calculation of the quantities τ_t , τ_l , and $(\partial f_0 / \partial t)_{sc}$.

Acoustic-Phonon Scattering

The relaxation time tensor for this type of scattering has been calculated by Herring and Vogt.³¹ The tensor components are frequently used in the form

$$(1/\tau_{ac\lambda}) = w_{ac\lambda} x^{1/2} (T/T_n)^{3/2}, \quad (17)$$

where $x = \epsilon/kT$ is the normalized electron energy. The symbol λ represents t or l .

The acoustic coupling constants w_{act} and w_{acl} are

³¹ C. Herring and E. Vogt, Phys. Rev. **101**, 944 (1955).

defined by

$$w_{ac\lambda} = \frac{3 \times 2^{5/2} \pi^3 m_i m_l^{1/2} (kT_n)^{3/2} \Xi_\lambda^2}{h^4 C_l}. \quad (18)$$

The "temperature" T_n appearing in (17) and (18) is a conveniently chosen normalization factor. C_l is the average elastic constant for longitudinal acoustic waves³¹:

$$C_l = \frac{1}{5}(3c_{11} + 2c_{12} + 4c_{44}). \quad (19)$$

Ξ_l and Ξ_l are simple functions of the deformation potentials Ξ_u and Ξ_d .³¹ Putting $\Xi_d/\Xi_u = r$, the results of Herring and Vogt can be written

$$\begin{aligned} \Xi_i^2 &= \Xi_u^2(1.31r^2 + 1.61r + 1.01) \\ \Xi_l^2 &= \Xi_u^2(1.24r^2 + 2.32r + 1.22) \end{aligned} \quad (20a)$$

for *n*-Ge.

In the case of *n*-Si we have³²

$$\begin{aligned} \Xi_i^2 &= \Xi_u^2(1.33r^2 + 1.15r + 1.07) \\ \Xi_l^2 &= \Xi_u^2(1.40r^2 + 2.40r + 1.62) \end{aligned} \quad (20b)$$

Using different averaging procedures, Samoilovich, Dakhovskii, and others^{33,34} have obtained numerical results which deviate slightly from those of Herring and Vogt.

The energy relaxation due to acoustic phonons has been analyzed in detail by Risken.³⁵ The result is

$$\left(\frac{\partial f_0}{\partial t}\right)_{ac} = w_{ac0} x^{-1/2} \frac{d}{dx} \left[x^2 \left(\frac{df_0}{dx} + f_0 \right) \right], \quad (21)$$

where

$$w_{ac0} = \frac{2^{11/2} \pi^3 m_i^2 m_l^{1/2} (kT)^{1/2} \Xi_0^2}{\rho h^4}. \quad (22)$$

Using $K_m = m_l/m_i$ and $r = (\Xi_d/\Xi_u)$, we can define Ξ_0 by

$$\Xi_0^2 = \Xi_u^2 \frac{2}{3} ((2 + K_m)r^2 + 2K_m r + K_m) \quad (23)$$

(valid for Ge as well as Si).

Scattering by Ionized Impurities

This type of scattering conserves the energy of the scattered electron, and it follows immediately that

$$(\partial f_0 / \partial t)_i = 0. \quad (24)$$

The relaxation-time formalism of Herring and Vogt is valid for energy-conserving scattering processes if the scattering anisotropy is not too large. This condition is in fact not very well fulfilled for impurity scattering in *n*-Ge. We have, however, applied the relaxation-time integrals of Herring and Vogt to this problem. The

³² C. Herring and E. Vogt, Phys. Rev. **105**, 1933 (1957).

³³ A. G. Samoilovich, I. Ya. Korenblit, I. V. Dakovskii, and V. D. Iskra, Fiz. Tverd. Tela **3**, 3285 (1961) [English transl.: Soviet Phys.—Solid State **3**, 2385 (1962)].

³⁴ I. V. Dakhovskii, Fiz. Tverd. Tela **5**, 2332 (1963) [English transl.: Soviet Phys.—Solid State **5**, 1695 (1964)].

³⁵ H. Risken, doctoral thesis, University of Aachen, 1962 (unpublished).

relaxation-time tensor derived in this manner should be sufficiently accurate for use in the case of dominating phonon scattering (consistent with our assumption of relatively small impurity concentrations).

As the relaxation times are required for use in numerical calculations only, the scattering integrals were calculated on a digital computer and simple analytic functions were fitted to the tabulated results. The impurity relaxation-time functions obtained by this approximation are

$$\frac{1}{\tau_{i\lambda}} \cong w_i x^{-3/2} \left[a_\lambda \ln(1 + (b_\lambda q x)^2) - \frac{c_\lambda}{1 + (d_\lambda/q x)^2} \right], \quad (25)$$

where λ stands for *t* or 1. The energy-independent factors w_i and q are defined by

$$w_i = \frac{3\pi e^4 N_I m_i}{2^{3/2} (4\pi\epsilon_0\kappa)^2 m_i^{3/2} (kT)^{3/2}}, \quad (26)$$

$$q = \frac{(4\pi\epsilon_0\kappa) 2\pi m_i (kT)^2}{e^2 h^2 n}. \quad (27)$$

N_I and n are the concentrations of impurities and electrons. κ is the relative dielectric constant of the crystal. The numerical factors of Eq. (25) are given in Table I for *n*-Si and *n*-Ge. Intervalley scattering by ionized impurities will become important at high impurity concentrations or low temperatures.³⁶ This mechanism will, however, be neglected here.

Optical-Phonon Scattering

Intravalley scattering by optical phonons is of importance in *n*-Ge but can be neglected in the case of *n*-Si.³⁷ As the scattering process is isotropic, we can use a simple scalar momentum relaxation time⁴:

$$\begin{aligned} \frac{1}{\tau_0} &= w_0 \left(\frac{T}{T_n} \right)^{1/2} \left(\frac{\Theta_0}{T_n} \right) \\ &\times [n_0(x+x_0)^{1/2} + (n_0+1)(x-x_0)^{1/2}]. \end{aligned} \quad (28)$$

TABLE I. Numerical values of the coefficients in Eq. (25). Calculated for $K_m = 20$ (Ge) and $K_m = 4.69$ (Si).

	λ	a_λ	b_λ	c_λ	d_λ
Si	<i>l</i>	1.059	1.226	1.200	4.97
	<i>t</i>	3.765	0.788	5.21	5.87
Ge	<i>l</i>	2.74	0.748	5.75	7.07
	<i>t</i>	34.7	0.324	83.6	9.95

³⁶ G. Weinreich, T. M. Sanders, and H. G. White, Phys. Rev. **111**, 747 (1958).

³⁷ W. A. Harrison, Phys. Rev. **104**, 1281 (1956).

Similarly the energy relaxation is described by⁴

$$\left(\frac{\partial f_0}{\partial t}\right)_0 = w_0 \left(\frac{T}{T_n}\right)^{1/2} \left(\frac{\Theta_0}{T_n}\right) \times \{ (x+x_0)^{1/2} [(n_0+1)f_0(x+x_0) - n_0f_0(x)] + (x-x_0)^{1/2} [n_0f_0(x-x_0) - (n_0+1)f_0(x)] \}. \quad (29)$$

Here w_0 is the coupling constant for optical phonons, $x_0 = \hbar\omega_0/kT = \Theta_0/T$ is the normalized phonon energy, and $n_0 = 1/(\exp x_0 - 1)$ is the occupation number. We are using the convention $(x-x_0)^{1/2} = 0$ for $x < x_0$. Finally, we define two parameters b_0 and a_0 expressing the ratio between optical- and acoustic-phonon scattering:

$$b_0 = w_0/w_{\text{act}}, \quad (30a)$$

$$a_0 = (w_0/w_{\text{ac0}})(T/T_n)^{1/2}(\Theta_0/T_n). \quad (30b)$$

(Both are independent of the arbitrary scaling factor T_n .) From (18) and (22) one gets

$$a_0 = b_0 \frac{3\rho\hbar\omega_0\Xi_t^2}{8C_t m_t \Xi_0^2}. \quad (31)$$

For n -Ge the energy of the active phonon is given by

$$\theta_0 = \hbar\omega_0/k = 430^\circ\text{K}.$$

Intervalley Scattering

We shall only consider intervalley scattering by phonons of high energy. In n -Ge longitudinal acoustic (LA) and longitudinal optic (LO) phonons with an equivalent temperature

$$\theta_2 = \hbar\omega_2/k = 315^\circ\text{K}$$

will give rise to intervalley transitions between equivalent valleys.^{36,38} Isotropic scattering equations in complete analogy with (28) and (29) can be used. The intervalley coupling constant w_2 has been determined from measurements by Weinreich *et al.*³⁶ The result is conveniently written³⁹

$$b_2 = w_2/w_{\text{act}} \cong 0.04. \quad (32)$$

Intervalley scattering in n -Si has been studied experimentally by Long.⁴⁰ It turns out that one must distinguish between “ f scattering” where electrons are transferred between two perpendicular valleys and “ g scattering” coupling two opposite valleys. The latter process can be treated as intravalley scattering in all calculations on transport phenomena because two parallel valleys may be considered as one single valley.

The g -type processes are caused by interaction with

LA phonons⁴¹ with an equivalent temperature.⁴⁰

$$\theta_g = \hbar\omega_g/k = 190^\circ\text{K},$$

and the f -type transitions occur by interaction with a phonon which is a mixture of the two modes LA and transverse optic (TO).⁴¹ The energy is given by⁴⁰

$$\theta_f = \hbar\omega_f/k = 630^\circ\text{K}.$$

Long defines a coupling constant w_1 for the 630°K phonon and another constant w_2 for the 190°K phonon. His experimental results are⁴⁰

$$b_1 = w_1/w_{\text{act}} \cong 2.0 \quad \text{and} \quad b_2 = w_2/w_{\text{act}} \cong 0.15.$$

More recent piezoresistance data seem to confirm these numerical values.⁴²

Electron-Electron Scattering

This type of scattering is not taken into account in our calculations. It should, however, be included if the electron density becomes significantly larger than 10^{14} cm^{-3} at 77°K or 10^{16} cm^{-3} at 300°K.¹⁰ Neglecting the e - e scattering may cause large errors in the values of the warm-electron parameters for $n \approx 10^{15}$ cm^{-3} at 77°K.⁴³

V. SOLUTION OF THE BOLTZMANN EQUATION

The warm-electron Boltzmann equation (13) will now be developed further for the electrons in a single valley. In the first approximation intervalley scattering is neglected. Later it will be included through the valley repopulation effect. In order to shorten the notation we introduce the function

$$h(x) = \tau_t(x)/\tau_{\text{act}}(x), \quad (33)$$

where $x = \epsilon/kT$ and $1/\tau_t = 1/\tau_{\text{act}} + 1/\tau_0 + 1/\tau_{it} + \dots$ (using the relaxation-time components defined in Sec. IV). Following the idea of Eq. (16) we shall write the distribution function in the form

$$f_0(x) = C_0 e^{-x} [1 + (\mathbf{F} \cdot \boldsymbol{\Omega} \cdot \mathbf{F}) y(x) / F_A^2]. \quad (34)$$

The normalization factor F_A is defined by

$$F_A^2 = \frac{3m_t k T w_{\text{act}} w_{\text{ac0}}}{2e^2} \left(\frac{T}{T_n}\right)^{3/2}. \quad (35)$$

Using (33), (34), and (35) and dropping higher-order field terms, we transform the basic equation (13) into

$$\left(\frac{\partial y}{\partial t}\right)_{\text{sc}} = w_{\text{ac0}} x^{-1/2} e^x \frac{d}{dx} (x e^{-x} h(x)), \quad (36)$$

which now has to be solved for $y(x)$.

³⁸ M. Lax, *Bull. Am. Phys. Soc.* **6**, 109 (1961).

³⁹ E. S. G. Paige, *Progr. Semicond.* **8** (1964).

⁴⁰ D. Long, *Phys. Rev.* **120**, 2024 (1960).

⁴¹ M. Lax and J. J. Hopfield, *Phys. Rev.* **124**, 115 (1961).

⁴² J. E. Aubrey, W. Gubler, T. Henningsen, and S. H. Koenig, *Phys. Rev.* **130**, 1667 (1963).

⁴³ J. Yamashita, *Progr. Theoret. Phys. (Kyoto)* **24**, 357 (1960)

The method of solution used in this work is described in some detail in Appendix I. It involves a simple numerical iteration procedure. In the following we shall assume that $y(x)$ has been computed and normalized so that the following equation is satisfied:

$$\int_0^{\infty} e^{-x} x^{1/2} y(x) dx = 0. \quad (37)$$

In a single valley, not interacting with other valleys, Eq. (37) expresses conservation of particles. When dealing with a many-valley model, we must add some energy-independent terms to $y(x)$ in order to account for the repopulation effects. This is discussed in Sec. VI.

VI. CALCULATION OF β_0 AND γ_0

In Sec. V and Appendix I we have derived the distribution function for a single valley, neglecting the intervalley scattering contributions. In a many-valley semiconductor we cannot, however, neglect the repopulation phenomena occurring even at extremely low intervalley scattering rates. For valley number ν we can express the distribution function by

$$f_0^{(\nu)}(x) = C^{(\nu)} e^{-x} [1 + (\mathbf{F} \cdot \boldsymbol{\Omega}^{(\nu)} \cdot \mathbf{F}) y(x) / F_A^2], \quad (38)$$

where $y(x)$ is the distribution function defined in Sec. V. The repopulation is taken into account by ascribing different values of $C^{(\nu)}$ to different valleys. Suppose that the major part of the intervalley transitions is caused by phonons of energy $\hbar\omega_2$. Now the principle of detailed balance requires the quantity

$$I = \int_0^{\infty} x^{1/2} [(x+x_2)^{1/2} n_2 + (x-x_2)^{1/2} (n_2+1)] f_0^{(\nu)}(x) dx \quad (39)$$

to be independent of ν . (n_2 is the phonon occupation number and $x_2 = \hbar\omega_2/kT$.) Inserting (38) into (39) one obtains after straightforward calculations the following proportionality:

$$I \propto C^{(\nu)} [1 + (\mathbf{F} \cdot \boldsymbol{\Omega}^{(\nu)} \cdot \mathbf{F}) B / F_A^2], \quad (40)$$

where the repopulation parameter B is defined by

$$B = \frac{\int_0^{\infty} x^{1/2} (x+x_2)^{1/2} e^{-x} [y(x+x_2) + y(x)] dx}{2 \int_0^{\infty} x^{1/2} (x+x_2)^{1/2} e^{-x} dx}. \quad (41)$$

At sufficiently low fields we have

$$(\mathbf{F} \cdot \boldsymbol{\Omega}^{(\nu)} \cdot \mathbf{F}) / F_A^2 \ll 1, \quad (42)$$

and it follows from (40) that $C^{(\nu)}$ can be written in the form

$$C^{(\nu)} = C(F) [1 - (\mathbf{F} \cdot \boldsymbol{\Omega}^{(\nu)} \cdot \mathbf{F}) B / F_A^2], \quad (43)$$

where $C(F)$ may depend on F but is independent of ν . The total number of electrons in the conduction band is proportional to

$$S = \frac{2}{\sqrt{\pi}} \sum_{\nu} \int_0^{\infty} x^{1/2} f_0^{(\nu)}(x) dx. \quad (44)$$

Now we can eliminate $C(F)$ by calculating S and using the fact that S must be independent of F . From (37), (38), and (42) we get

$$S = C(F) N_{\nu} \left[1 - B \left(\frac{F}{F_A} \right)^2 \frac{2K+1}{3K} \right]. \quad (45)$$

Here we have used a simple relation describing summation over a complete set of $\langle 111 \rangle$ or $\langle 100 \rangle$ valleys:

$$\sum_{\nu} \mathbf{e} \cdot \boldsymbol{\Omega}^{(\nu)} \cdot \mathbf{e} = N_{\nu} (2K+1) / 3K, \quad (46)$$

where N_{ν} is the number of valleys and \mathbf{e} is an arbitrary unit vector. It follows from (45) that $C(F)$ must have the form

$$C(F) = C_0 \left[1 + B \left(\frac{F}{F_A} \right)^2 \frac{2K+1}{3K} \right]. \quad (47)$$

Finally we obtain the expression for the distribution in the ν th valley:

$$f_0^{(\nu)}(x) = C_0 e^{-x} \left[1 + \left(F^2 B \frac{2K+1}{3K} + (\mathbf{F} \cdot \boldsymbol{\Omega}^{(\nu)} \cdot \mathbf{F}) (y(x) - B) \right) / F_A^2 \right]. \quad (48)$$

Now the warm-electron parameters β_0 and γ_0 can be determined. The calculations are given in Appendix II. The result is

$$\beta_0 = \frac{(2K+1)D}{3KF_A^2}, \quad (49)$$

$$\gamma_0 = \frac{2(K-1)^2(B-D)}{3K(2K+1)F_A^2}.$$

The scattering parameter D is defined by

$$D = \frac{\int_0^{\infty} x e^{-x} h(x) [y(x) - dy/dx] dx}{\int_0^{\infty} x e^{-x} h(x) dx}. \quad (50)$$

Equation (49) is valid for a many-valley semiconductor with $\langle 111 \rangle$ minima, if the intervalley scattering is sufficiently weak.

A similar argument can of course be applied to a many-valley structure with $\langle 100 \rangle$ minima. For completeness we shall quote the result (in spite of the fact that the assumption of weak intervalley scattering is in

general not true for Si):

$$\beta_0 = \left(\frac{2K+1}{3K} D + \frac{2(K-1)^2}{3K(2K+1)} (D-B) \right) / F_A^2, \quad (51)$$

$$\gamma_0 = \frac{(K-1)^2(D-B)}{K(2K+1)F_A^2}.$$

Of special interest are the field directions where the valleys are equally oriented with respect to the field vector ($\langle 100 \rangle$ for Ge and $\langle 111 \rangle$ for Si). In this case all valleys have the same distribution function $f_0(x)$, and we are essentially dealing with a one-valley problem where intervalley scattering can be treated exactly like optical intervalley scattering. The value of the β function in these directions of high symmetry is

$$\beta_{\text{sym}} = (2K+1)D/3KF_A^2. \quad (52)$$

VII. EXPERIMENTAL METHOD

The coefficient β of Eq. (3) was determined from a measurement of the nonlinear distortion in the crystals by the method of Guldbrandsen *et al.*²⁸ A simplified diagram of the measuring circuit is shown in Fig. 2(a). An audio-frequency sine wave is applied to the sample, and the first harmonic as well as the higher harmonics from the generator and the transformer are balanced out by a simple bridge circuit, so that only the higher harmonics generated in the sample remain at the input terminals of the selective voltmeter. Denoting the rms values of the sample voltage and the third harmonic output voltage by V_1 and V_3 respectively, we have

$$|\beta| = 4L^2 V_3 / V_1^3, \quad (53)$$

where L is the length of the crystal. As the bridge circuit can be operated with an extreme degree of accuracy²⁸ we are left with two major sources of error: (a) Joule heating of the crystal and (b) non-Ohmic behavior of the sample contacts.

The Joule heating of the crystal lattice will generate temperature oscillations with the frequency 2ω . The corresponding modulation of conductivity will give rise to an additional third harmonic signal which is about 90° out of phase with respect to the warm-electron

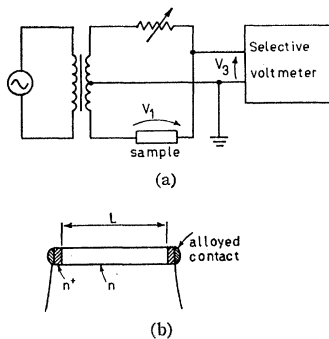


FIG. 2. (a) Schematic diagram of measuring circuit. (b) Sample geometry.

signal. This effect will introduce an error which can be computed with reasonable accuracy. The numerical value of β will be increased by the amount

$$\delta\beta = \frac{1}{2\omega^2} \left[\frac{1}{|\beta|} \left(\frac{\alpha\sigma_0}{2\rho CT} \right)^2 + \frac{\alpha\sigma_0}{2\rho CT t_c} \right], \quad (54)$$

where T is the lattice temperature, C the specific heat, and ρ the density of the crystal. t_c is a time constant describing the rate of heat exchange between the crystal and its surroundings. The dimensionless factor α shall account for the temperature dependence of the conductivity: $\sigma_0 \propto T^{-\alpha}$.

It turns out that $\delta\beta$ will be negligible for high Ohmic crystals, when the operating frequency ω exceeds a few kc/sec.

Injection of minority carriers from the electric contacts is avoided by using a special sample geometry with low-Ohmic zones at the ends of the crystal, as suggested by Schmidt-Tiedemann⁴⁴ (Fig. 2b). The Ohmic contacts are made by alloying Au with 0.4% Sb to the highly doped ends of the sample. This technique applies well to n -Si as well as n -Ge. The performance of the contacts is satisfying between 77 and 250°K for Si. In the case of Ge, however, some of the contacts showed a nonlinear distortion signal comparable to the β signal, when the temperature exceeded 150°K. The quality of the contacts can be estimated from a measurement of the second harmonic generated by the sample (assuming that the two contacts are not exactly identical).

VIII. NUMERICAL RESULTS

In this section experimental data are presented together with the results from theoretical calculations.

n -Type Si

The theory developed in the preceding sections is in general not valid for silicon because of the strong (f -type) intervalley scattering between perpendicular valleys. We can, however, use the theory without restrictions in two special cases. The most obvious of these is the case of $\langle 111 \rangle$ -oriented samples, where (because of symmetry) the intervalley scattering can be treated like optical intravalley scattering. Figure 3 illustrates the comparison between theory and experiment for two $\langle 111 \rangle$ samples cut from a 40- Ω cm crystal. Also, Fig. 3 shows data obtained from a microwave experiment by Hamaguchi *et al.*²⁷ (crystal orientation not specified).

The curves were calculated from Eq. (52) using Long's relative intervalley coupling constants.⁴⁰ In the calculation of coupling constants for acoustic-phonon scattering a fixed value of the ratio $(\Xi_d/\Xi_u) = -0.05$ was used. (This is consistent with Long's analysis of scattering anisotropy.⁴⁰ The results are not very sensitive to the choice of this constant.) We assume $K \cong K_m = 4.69$.

⁴⁴ K. J. Schmidt-Tiedemann, Physik. Verhandl. 9, 150 (1960).

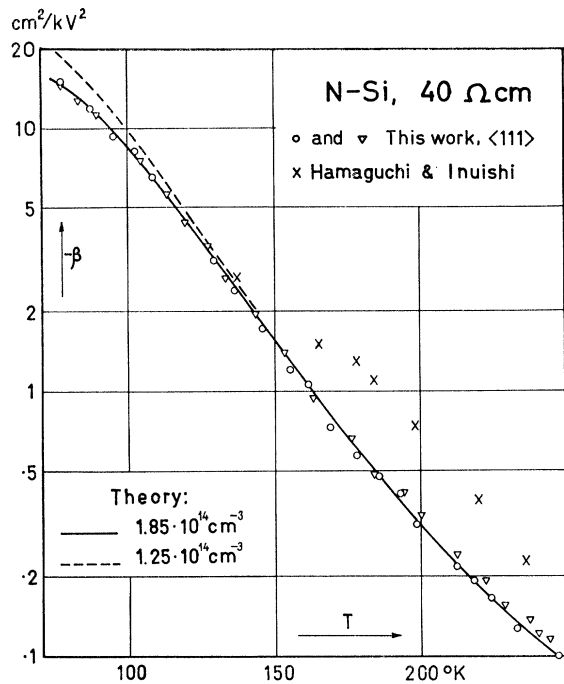


FIG. 3. Warm-electron coefficient β as a function of lattice temperature T for 40- Ω cm *n*-Si. The points are experimental. The solid curve was calculated for $N_I = 1.85 \times 10^{14}$ cm $^{-3}$. The broken curve corresponds to $N_I = 1.25 \times 10^{14}$ cm $^{-3}$.

By varying the input values of $\bar{\mathcal{E}}_u$ and N_I the best fit to the experimental points was obtained for $\bar{\mathcal{E}}_u = 8.4$ eV and $N_I = 1.85 \times 10^{14}$ cm $^{-3}$. This fitting procedure is very sensitive to the choice of $\bar{\mathcal{E}}_u$ and the value 8.4 eV is in good agreement with independent experiments.⁴⁵

The carrier concentration calculated from room-temperature resistivity is about 1.25×10^{14} cm $^{-3}$. An ionized impurity concentration $N_I = 1.85 \times 10^{14}$ cm $^{-3}$ could be explained by assuming a slight degree of compensation.

When experimental uncertainties are taken into account, we must conclude that the agreement between theory and experiment is satisfying.

There is another special case in which our theory should apply to *n*-Si over quite a large temperature range. Consider a crystal to which a very high uniaxial pressure is applied along the $\langle 100 \rangle$ direction. At sufficiently high pressure the carriers will concentrate completely in the two valleys which are parallel to the pressure axis. Under these conditions we are dealing with a one-valley problem, and the warm-electron coefficient for the stressed crystal will not be influenced by f scattering.

The results of such an experiment and a comparison with theory has been published elsewhere.²⁹ Also here the theoretical curves can be fitted to the experimental data. One must, however, use a rather low value of the deformation potential constant: $\bar{\mathcal{E}}_u = 7.5$ eV. This dis-

⁴⁵ I. Balslev, Phys. Rev. 143, 636 (1966).

crepancy might be due to a stress-dependent effective mass,⁴⁶ which has not been taken into account in our calculations.

n-Type Ge

The assumption of weak intervalley scattering should be well fulfilled for pure germanium in the temperature range 77–250°K. It follows that our theory will enable us to calculate β_0 as well as γ_0 (or to calculate β for an arbitrary sample orientation).

β has been measured as a function of temperature for 10- Ω cm *n*-Ge. The results are shown in Fig. 4 for two different sample orientations: $\alpha = 0^\circ$ and $\alpha = 72^\circ$. Experimental data of Hamaguchi *et al.*²⁷ are shown in Fig. 4 for comparison. (Crystal orientation is not specified.) The theoretical curves in Fig. 4 were fitted to the experimental points by varying the ratio $(\bar{\mathcal{E}}_d/\bar{\mathcal{E}}_u)$ and the relative coupling constant b_0 which indicates the strength of optical-phonon scattering. For the remaining parameters the following fixed values were used: $N_I = 2 \times 10^{14}$ cm $^{-3}$ (estimated from the resistivity); $b_2 = 0.04$ (from Weinreich *et al.*^{36,39}); $K = K_m = 20$; $\bar{\mathcal{E}}_u = 18$ eV (deduced from different piezoresistance measurements³⁹ (77°K)). The best fit is obtained for $(\bar{\mathcal{E}}_d/\bar{\mathcal{E}}_u) = -0.34$ and $b_0 = 0.17$. Both values are in reasonable agreement with the generally accepted data on *n*-Ge.³⁹

It should be noted that a possible temperature de-

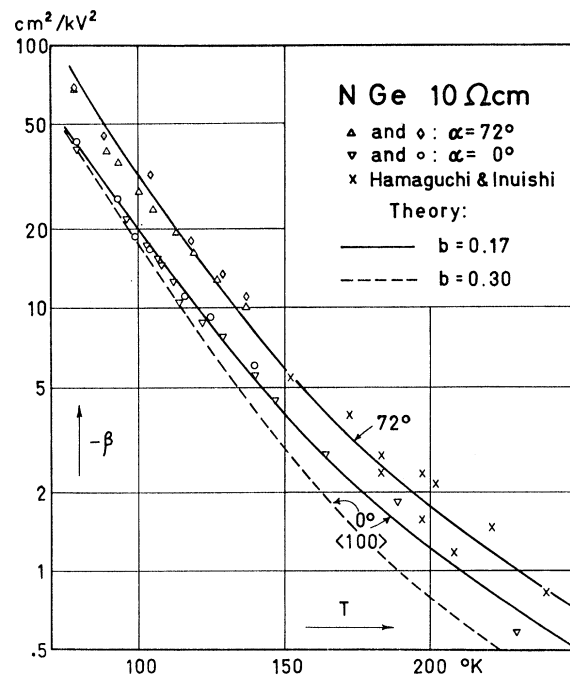


FIG. 4. The experimental points show β versus T for 10- Ω cm *n*-Ge samples with different orientations. The solid curves were calculated for $b_0 = 0.17$ with $\alpha = 0^\circ$ and $\alpha = 72^\circ$, respectively. The broken curve corresponds to $b_0 = 0.30$ and $\alpha = 0^\circ$.

⁴⁶ J. C. Hensel, H. Hasegawa, and M. Nakayama, Phys. Rev. 138, A225 (1965).

pendence of Ξ_u ³⁹ has not been considered in these calculations. Such an effect would influence the b_0 value obtained by the fitting procedure. A detailed discussion of this problem is considered to be outside the scope of this treatment.

IX. CONCLUSION

We have seen that the warm-electron distribution function can be calculated numerically for any combination of scattering mechanisms, when only one isolated valley is considered. It was shown that a calculation of β can be based on the one-valley solution, even in the case of strong intervalley scattering, provided that the field vector is parallel to a suitable symmetry axis. A general solution of the warm-electron Boltzmann equation (calculation of β_0 and γ_0) was carried out for n -Ge under the assumption of sufficiently weak intervalley scattering, so that the interaction between electron distributions in different valleys could be accounted for by a simple valley repopulation argument.

Experimental results were obtained from the analysis of nonlinear distortion in the crystals at low-power levels.

The theory was tested by comparison with the measurements for pure n -Si and n -Ge. Using Long's data on intervalley scattering in Si we found that the value for Ξ_u to be used in the acoustic scattering terms was 8.4 eV.

Assuming the value $\Xi_u = 18$ eV to be valid for Ge, one found by fitting the theoretical curves to the experimental data ($\Xi_a/\Xi_u = -0.34$ and $b_0 = 0.17$).

ACKNOWLEDGMENTS

The author is greatly indebted to Professor N. I. Meyer for valuable advice and encouragement during all stages of this work. Thanks are due to T. Gulbrandsen and J. Schær-Jakobsen for designing important parts of the electronic equipment and to E. Mosekilde for helpful experimental suggestions and assistance with the measurements. The computer facilities were kindly provided by the Northern Europe University Computing Center (NEUCC).

APPENDIX I: CALCULATION OF $y(x)$

As an illustration of the method of solution, consider the case of n -Ge where $(\partial y/\partial t)_{sc}$ can be expressed essentially as a sum of the scattering terms for acoustic and optical phonons. Combining (21), (29), (30b), and (34) gives

$$\begin{aligned} (\partial y/\partial t)_{sc} = w_{ac0} \left\{ e^{x_0} x^{-1/2} \frac{d}{dx} \left[e^{-x} x^2 \frac{dy}{dx} \right] \right. \\ \left. + a_0 n_0 [(x+x_0)^{1/2} (y(x+x_0) - y(x)) \right. \\ \left. + e^{x_0} (x-x_0)^{1/2} (y(x-x_0) - y(x)) \right] \}. \quad (55) \end{aligned}$$

Inserting (55) into (36) and substituting a new function:

$$z(x) = x(dy/dx) \quad (56)$$

one obtains

$$\begin{aligned} \frac{d}{dx} [x e^{-x} (h(x) - z(x))] = a_0 n_0 e^{-x} x^{1/2} \\ \times \left[(x+x_0)^{1/2} \int_x^{(x+x_0)} \frac{z(r) dr}{r} \right. \\ \left. - e^{x_0} (x-x_0)^{1/2} \int_{(x-x_0)}^x \frac{z(r) dr}{r} \right]. \quad (57) \end{aligned}$$

[Here and in the following the expression $(x-x_0)$ has to be replaced by 0 for $x < x_0$.] Equation (57) is now integrated (from 0 to x) and finally multiplied by e^x/x , and we obtain the final Boltzmann equation:

$$h(x) - z(x) = \hat{L}_0 z(x), \quad (58)$$

where the optical scattering operator \hat{L}_0 has been defined by

$$\begin{aligned} \hat{L}_0 z(x) = \frac{a_0 n_0 e^x}{x} \int_{(x-x_0)}^x ds e^{-s} (s+x_0)^{1/2} s^{1/2} \\ \times \int_s^{(s+x_0)} \frac{z(r) dr}{r}. \quad (59a) \end{aligned}$$

If several high-energy phonons contribute to the scattering, Eq. (58) is immediately generalized by adding on the right side new terms of the form

$$\begin{aligned} \hat{L}_i z(x) = \frac{a_i n_i e^x}{x} \int_{(x-x_i)}^x ds e^{-s} (s+x_i)^{1/2} s^{1/2} \\ \times \int_s^{(s+x_i)} \frac{z(r) dr}{r}. \quad (59b) \end{aligned}$$

An analytic solution of (58) does not seem possible. One can be guided to a simple numerical iteration method by the following argument.

Let $\xi(x,t)$ be a time-dependent distribution function obeying the equation

$$\frac{\partial \xi}{\partial t} = h(x) - \xi(x,t) - \hat{L}_0 \xi(x,t). \quad (60)$$

When an initial distribution $\xi(x,0)$ is chosen, $\xi(x,t)$ is uniquely determined by (60) for $t > 0$. If (60) leads to a stationary distribution $\xi(x,\infty)$, which is independent of the initial conditions as specified by $\xi(x,0)$, then the function $z(x) = \xi(x,\infty)$ will be the solution to the warm-electron Boltzmann equation (58).

It is not difficult to find the stationary solution to (60) by iteration. One may choose an arbitrary function $z_0(x)$ and calculate

$$\begin{aligned} z_1(x) &= z_0(x) + \Delta t [h(x) - z_0(x) - \hat{L}_0 z_0(x)], \\ z_2(x) &= z_1(x) + \Delta t [h(x) - z_1(x) - \hat{L}_0 z_1(x)], \\ &\vdots \\ z_n(x) &= z_{n-1}(x) + \Delta t [h(x) - z_{n-1}(x) - \hat{L}_0 z_{n-1}(x)]. \end{aligned} \quad (61)$$

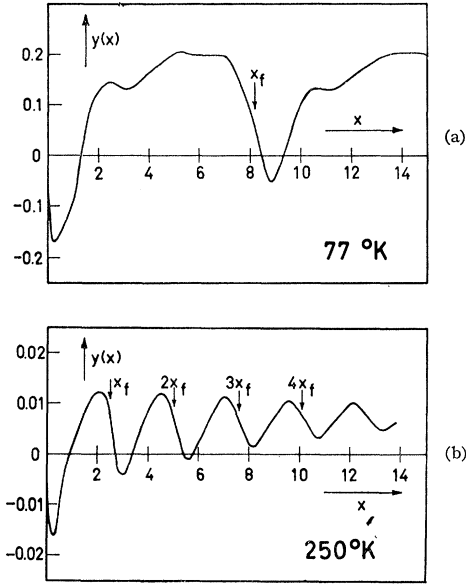


FIG. 5. Warm-electron distribution function y as a function of $x = \epsilon/kT$. Computed for 40- Ω cm *n*-Si at two different lattice temperatures: (a) 77°K and (b) 250°K. The normalized phonon energy $x_f = \hbar\omega_f/kT$ is indicated.

(This operation may also be interpreted as an integration with respect to the time variable t .)

The convergence is rapid, when a_0 is not too large. In the case of *n*-Ge ($a_0 \approx 40$) about 15 steps are required to give an over-all accuracy of 0.5%. The convergence and the stability strongly depend, however, on the choice of the step length Δt . A very small, constant value of Δt will, of course, ensure perfect stability, but the number of steps required will under these conditions become prohibitively large. Consequently a procedure was developed which allows the computer to determine the optimal value of Δt before each step is taken. This operation involves a detailed analysis of the results obtained during the preceding steps.

After a short inspection of Eqs. (59a) and (59b) one might anticipate that the numerical evaluation of the double integral in the optical term would demand too much computer time, but it turns out that the optical scattering term can be tabulated quite rapidly by proper arrangement of the arithmetical operations.

When the stationary solution $z(x)$ has been tabulated, $y(x)$ is found by numerical integration of (56) and

normalized according to Eq. (37), and the integrals in (41) and (50) are evaluated numerically.

Figure 5 shows the distribution function $y(x)$ as calculated for 40- Ω cm *n*-Si at two different lattice temperatures: (a) 77°K and (b) 250°K. There is an obvious correlation between the detailed shape of the curves and the energy of the dominating (f -type) phonon.

APPENDIX II: CALCULATION OF β_0 AND γ_0

From Eq. (14) we derive the following proportionality for the longitudinal current component:

$$J_L \propto F \sum_{\nu} (\mathbf{e} \cdot \boldsymbol{\Omega}^{(\nu)} \cdot \mathbf{e}) \int_0^{\infty} x h(x) e^{-x} \left(\frac{df_0^{(\nu)}}{dx} \right) dx, \quad (62)$$

where the unit vector \mathbf{e} is defined by $\mathbf{e} = \mathbf{F}/F$. Combining (48) and (62) we get

$$J_L \propto F \sum_{\nu} (\mathbf{e} \cdot \boldsymbol{\Omega}^{(\nu)} \cdot \mathbf{e}) \left\{ 1 + \left(\frac{F}{F_A} \right)^2 \times \left[B \left(\frac{2K+1}{3K} \right) + (\mathbf{e} \cdot \boldsymbol{\Omega}^{(\nu)} \cdot \mathbf{e})(D-B) \right] \right\}, \quad (63)$$

where the scattering parameter D is defined in Eq. (50). In the case of *n*-Ge the summation in (63) has to be performed over a set of $\langle 111 \rangle$ valleys. Using Eq. (46) together with the following geometrical relation:

$$\sum_{\langle 111 \rangle} (\mathbf{e} \cdot \boldsymbol{\Omega}^{(\nu)} \cdot \mathbf{e})^2 = N_{\nu} \left\{ 1 - 2 \left(\frac{K-1}{3K} \right) + \left(\frac{K-1}{3K} \right)^2 (3 - 2 \sum_i e_i^4) \right\}, \quad (64)$$

one obtains

$$J_L \propto F \left\{ 1 + \left(\frac{F}{F_A} \right)^2 \left[D \left(\frac{2K+1}{3K} \right) - \frac{2(B-D)(K-1)^2}{3K(2K+1)} (1 - \sum_i e_i^4) \right] \right\}. \quad (65)$$

A simple comparison between (65) and the symmetry relation (4) will give us the expressions for β_0 and γ_0 shown in Eq. (49).